Design and Thermal Characteristics of a Synthetic Jet Ejector Heat Sink

Raghav Mahalingam[1]
e-mail: raghav.mahalingam@me.gatech.edu

Ari Glezer
e-mail: ari.glezer@me.gatech.edu

Fluid Mechanics and Heat Transfer Research Labs, George W. Woodruff School of Mechanical Engineering, Georgia Institute of Technology, Atlanta, GA 30332

The design and thermal performance of a synthetic-air-jet-based heat sink for high-power dissipation electronics is discussed. Each fin of a plate-fin heat sink is straddled by a pair of two-dimensional synthetic jets, thereby creating a jet ejector system that entrains cool ambient air upstream of the heat sink and discharges it into the channels between the fins. The jets are created by periodic pressure variations induced in a plenum by electromagnetic actuators. The performance of the heat sink is assessed using a thermal test die encased in a heat spreader that is instrumented with a thermocouple. The case-to-ambient thermal resistance under natural convection with the heat sink is 3.15°C/W. *Forced convection with the synthetic jets enables a power dissipation of* 59.2 W *at a case temperature of* 70°C, *resulting in a case-to-ambient thermal resistance of* 0.76°C/W. *The synthetic-jet heat sink dissipates ~40% more heat compared to steady flow from a ducted fan blowing air through the heat sink. The synthetic jets generate a flow rate of 4.48 CFM through the heat sink, resulting in 27.8 W/CFM and thermal effectiveness of 0.62. The effect of fin length on the thermal resistance of the heat sink is discussed. Detailed measurements on an instrumented heat sink estimate that the average heat transfer coefficients in the channel flow between the fins is 2.5 times that of a steady flow in the ducts at the same Reynolds Number.* [DOI: 10.1115/1.1869509]

1 Introduction

The rise in power dissipation levels of microprocessors accompanied by a shrinking thermal budget has resulted in the need for advanced cooling solutions. The *International Technology Roadmap for Semiconductors* [1] predicts a junction-ambient thermal resistance requirement of 0.33°C/W for cost performance computers by 2010. The steep cooling requirements have prompted development of two-phase and pumped liquid cooling techniques and it is perceived that even consumer systems will eventually need to use fluids other than air for cooling. However, in a recent review of the advances in electronics cooling, Bar-Cohen [2] noted that while two-phase and liquid cooling have potential for very high heat-removal requirements, consumer-oriented systems have focused on air cooling due to its simplicity. It appears that until liquid or two-phase cooling concepts reach a stage at which they can be reliably packaged, air cooling will continue to be the primary choice for thermal designers. In order to achieve the ever increasing power dissipation levels with current fan-heat-sink combinations, designers are being forced to use copper heat sinks or aluminum heat sinks with copper inlays as well as larger fans driving higher flow rates. While fans are capable of supplying ample volume flow rate, they are hindered by noise, long-term reliability, and low thermal effectiveness. Arrays of air-jets impinging on the heated surfaces can be used as an alternative to fans, but conventional air-jets are not very useful for consumer products, due to air supply and plumbing requirements.

Synthetic or "zero-mass-flux" jets (Smith and Glezer [3]), unlike conventional jets, require no mass addition to the system, and thus provide means of efficiently directing airflow across a heated surface. Synthetic jets are formed by periodic suction and ejection of fluid out of an orifice bounding a cavity by the time periodic motion of a diaphragm that is built into one of the walls of the cavity. Since synthetic jets are comprised entirely of the ambient fluid, they can be conveniently integrated with surfaces that require cooling, without the need for complex plumbing. The evolution of a synthetic jet and its interaction with a crossflow has been reviewed by Glezer and Amitay [4]. Synthetic jets are formed by a train of vortical structures and have far-field properties (e.g., rate of lateral spreading and streamwise decay of centerline velocity) that are similar to conventional turbulent jets.

While there is extensive literature on direct air cooling using fans and conventional jets [5–9], the concept of using synthetic jets for heat transfer is relatively new. It was demonstrated by Thompson et al. [10] that integrated cooling of single- and multichip modules could be achieved using synthetic-jet technology. They observed a 250% increase in power dissipation over natural convection for normal impingement cooling of a horizontal, 49-element metal-oxide semiconductor field-effect transistor multichip module using a single 1.6 mm round jet. Russell [11] showed that heat transfer from a surface could be enhanced by the coupling of a local side-blowing synthetic jet with a global flow. He also showed that an order of magnitude higher flow rate would be needed to achieve comparable cooling with just a fan-driven flow. Recently, Mahalingam and Glezer [12] demonstrated an active heat sink based on a normally impinging synthetic jet for moderate power dissipation requirements. In preliminary work related to the current study Mahalingam and Glezer [13] developed an integrated active heat sink based on synthetic jets for heat dissipation at power levels over 100 W at flow rates of about 3–4 CFM.

The present work focuses on the development of an active air-cooled heat sink based on the synthetic-jet ejector principle. Section 2 describes the experimental setup including the design of the heat sink. Section 3 discusses thermal performance of the heat sink. Section 4 presents the conclusions from this work.

2 Heat Sink Design and Experimental Setup

2.1 Synthetic Jet Ejector Heat Sink. The principle of jet ejectors or jet pumps [8,9] has been known for several decades. A jet ejector consists of a primary high momentum synthetic jet driving a secondary airflow through a channel, as shown in Fig. 1. The low pressure created by a primary jet discharging into the

[1]Phone: (404) 385-1892, Fax: (404) 894-8496

Contributed by the Electronic and Photonic Packaging Division for publication in the JOURNAL OF ELECTRONIC PACKAGING. Manuscript received January 27, 2003; revision received December 23, 2004. Review conducted by: D. Agonafer.

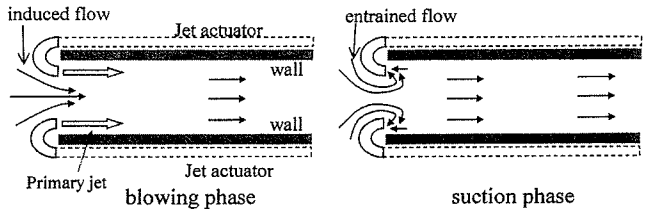

Fig. 1 Basic principle of operation of a synthetic jet ejector

channel results in entrainment of quiescent ambient flow, thus creating an increase in overall flow rate at the channel exit. In conventional jet ejectors, the primary jet is created using a pressure source ducted into the entry of a channel. The use of synthetic jets as the primary jet is an attractive option since the only input to the primary jet is electrical, requiring no plumbing and pressure supplies. In addition synthetic jets are attractive due to the ease of incorporating a jet module in low-profile compact geometries. During the blowing stroke of the primary synthetic jet, the jet ejector phenomenon is similar to steady jet ejectors, wherein a primary high-momentum jet creates a low pressure in a channel, resulting in the entrainment of fluid from the secondary quiescent medium. During the suction stroke, the low pressure in the jet cavity results is considerably higher secondary flow entrainment, which is forced out during the subsequent blowing stroke.

The concept described above can be scaled up to build a synthetic-jet ejector heat sink, a schematic diagram of which is shown in Fig. 2. The dimensions of the heat sink are nominally 120 mm × 70 mm × 30 mm. The top part in Fig. 2 shows the sectional side view of the heat sink, consisting of a L-shaped plate-fin (shaded gray) straddled by the synthetic-jet actuator. The plate-fin is cooled by two arrays of synthetic jets; one array is directed through the longer fins (labeled #1f) via nozzles connected to the plenum. The second array of jets is directed over the shorter fins (labeled #2f). The integrated circuit is shown attached to the base of the heat sink. The bottom part (sectional top-view) in Fig. 2 shows a horizontal section of the nozzles and a single channel formed by adjacent fins. The entire heat sink is made of 17 such channels. There is an additional fin in the center of each channel in order to increase the surface area exposed to the cooling flow. As seen in the sectional top-view and described in the previous

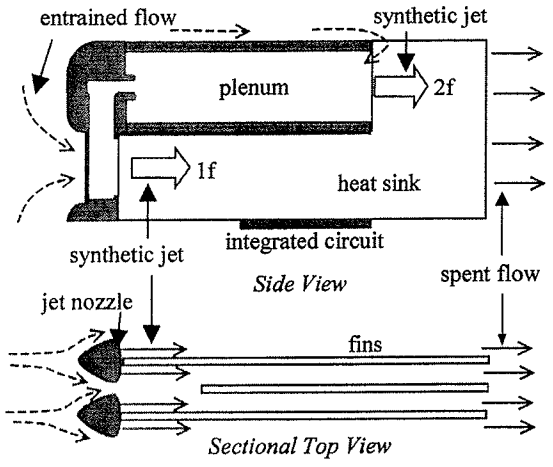

Fig. 2 Schematic diagram of the synthetic jet heat sink. A single channel is shown for clarity in the bottom figure. The module consists of 17 identical channels, with addition shorter fins within each channel to increase the surface area.

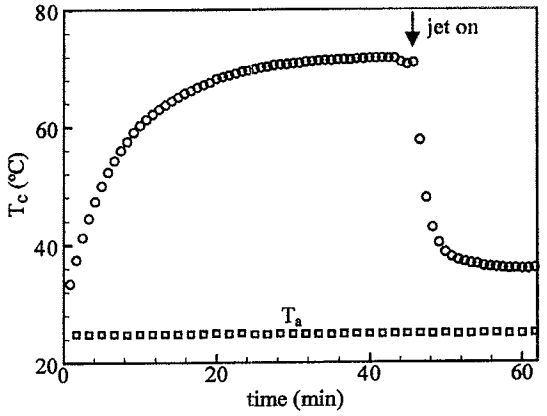

Fig. 3 Rapid cooling capability of synthetic jet ejector heat sink

paragraph, the jet flow induces a secondary flow (dashed arrows) of cooler air upstream of the nozzle that is heated up along the fins before exiting from the channels.

2.2 Test Setup and Uncertainties. A thermal test die having an area of 1.61 cm^2 encased in a copper heat spreader of 7.38 cm^2 area is used to assess the performance of the heat sink, which is attached to the copper heat spreader using screws through the substrate. Thermal grease is used to minimize contact resistance between the heat spreader and heat sink. The substrate is bonded to an insulating base of nylon embedded in foam in order to maximize the heat flow to the heat sink. Based on temperature measurements within the substrate it is estimated that under forced convection 5% of the total input power to the die is dissipated through the substrate and insulation. The case temperature of the thermal die is monitored using a T-type thermocouple having a bead of 0.25 mm diameter embedded in the center of the copper heat spreader. The air temperature is measured using a thermocouple that can be traversed along the length the center channels. The thermocouple readings are digitized using an 12-bit A/D board (National Instruments AT-MIO-16DE10) and cold-junction compensation is performed using an integrated circuit sensor embedded in the shielded I/O connector block (SCB-100), which is used as the interface between the A/D board and the thermocouple sensors. The measurements have a resolution of 0.024% of full scale, resulting in a temperature resolution of 0.03°C, since the temperature limits were set to 120°C. The maximum error for each temperature reading is no greater than ±1.5°C, which corresponds to an error of ±1.5–6% for the temperature range associated with the reported data (±6% error for an ambient temperature reading of 25°C and ±1.5% for a case temperature reading of 100°C). The flow at the exit of the heat sink is measured using a pitot static probe having an outer diameter of 0.8 mm, which results in 1% flow blockage based on the exit area of each channel. The pitot probe is connected to a 0.2 Torr Barocel™ pressure transducer with a full range output of 1.0 V, and the voltage output is digitized by the same A/D board described above, resulting in a resolution of 0.1 m/s and an accuracy of ±0.7% in the velocity measurements.

3 Results and Discussion

3.1 Thermal Performance. The rapid cooling capability of synthetic jets is measured by monitoring the case temperature continuously during testing and is shown in Fig. 3. With the heat sink and the synthetic jet module attached, the package reaches a steady state temperature of 71.5°C at a die power of 14.1 W under natural convection in approximately 45 min. Within 4 min of turning the synthetic jet on, T_c drops rapidly to ≈36°C. Thus,

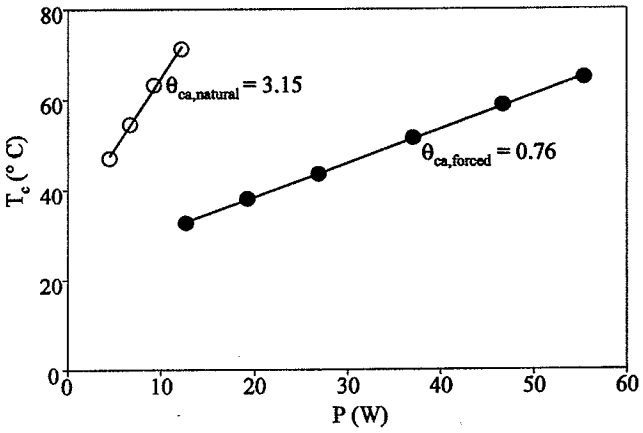

Fig. 4 Comparison of synthetic jet and natural convection (○) natural convection, (●) synthetic jet)

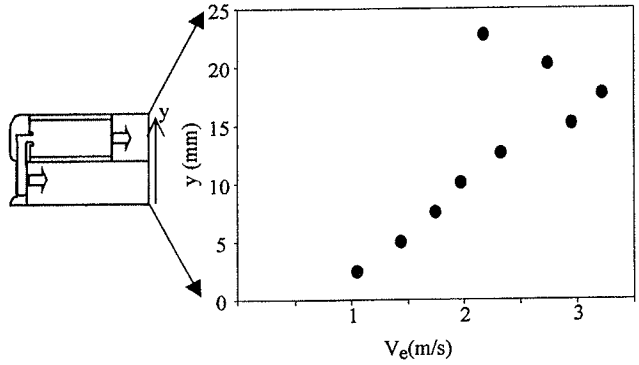

Fig. 6 Variation of exit velocity along the height of the channel

the rise in case temperature above ambient at constant power with the synthetic jets is approximately one-quarter of that under natural convection. Since the frequency of operation of the jets is around 250 Hz, resulting in a time period of 5 ms and the thermal time constant of the system is five orders of magnitude higher, a steady state temperature is attained without any fluctuations in case temperature.

The variation in power dissipated by natural and synthetic jet convection as a function of case temperature is shown in Fig. 4. The slope yields the case-to-ambient thermal resistance for the heat sink. Under natural convection, this corresponds to a thermal resistance, $\theta_{ca,natural}$=3.15°C/W. This thermal resistance includes the losses through the substrate (20%) and radiation (12%). Thus, the actual thermal resistance through the heat sink is only 4.63°C/W. With the synthetic-jet module mounted on the heat sink and the actuators operating at their optimum frequency and amplitude, the system dissipates 59.2 W at T_c=70°C, resulting in a nominal thermal resistance $\theta_{ca,forced}$=0.76°C/W. Note that this value includes the heat dissipated through the substrate (5%) and radiation (3%). Thus, the actual heat dissipated by the forced convection is 0.83, which is 457% more than under natural convection. It is worth noting that even though the jets entrain ambient fluid during the suction cycle, the increased local surface temperature of the fins does not deteriorate the performance of the jets. This can be attributed to the entrainment of cool ambient air due to the jet ejector effect.

The effectiveness of synthetic jets compared to the steady flow generated by a ducted fan is shown in Fig. 5, where the variation of power dissipated at T_c=100°C as a function of the flow rate is shown. All the flow generated by the fan was forced to pass through the heat sink by placing a duct from the fan to the heat sink. The flow rate was measured at the exit of the heat sink. The synthetic-jet device dissipates about 20–40% more power than a fan in the 3–5 CFM range, demonstrating the effectiveness of using synthetic jets at low flow rates.

3.2 Thermal Effectiveness of Heat Sink. The variation of exit velocity along the height of the channel is measured using a pitot probe at the exit section of the heat sink and is shown in Fig. 6. The data shown here are averaged from measurements in 12 channels spaced equally across the heat sink. The velocities at the bottom of the channel are lower than the top for two reasons. First, near the top of the channels the measurement locations are physically closer to the jet exit plane and thus the jet velocities will have decayed lesser than the bottom of the channels. Secondly, the flow near the bottom of the channels experiences higher drag due to the longer fins as well as the presence of the base plate. The overall flow rate obtained from these measurements is 4.7 CFM, which is equal to 0.27 CFM per fin pair.

The air temperature along one of the center channels of the heat sink is measured in order to determine the effective length beyond which the air is heated up to capacity and cannot absorb any more heat and to calculate the thermal effectiveness of the heat sink.

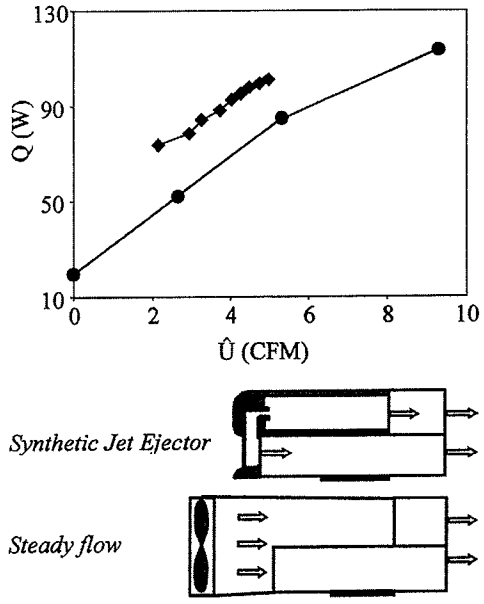

Fig. 5 Comparison of the thermal performance of synthetic jets (♦) and steady fan driven flow (●)

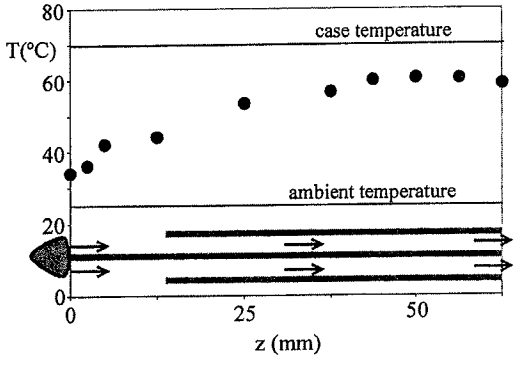

Fig. 7 Air temperature along the center channel of the heat sink

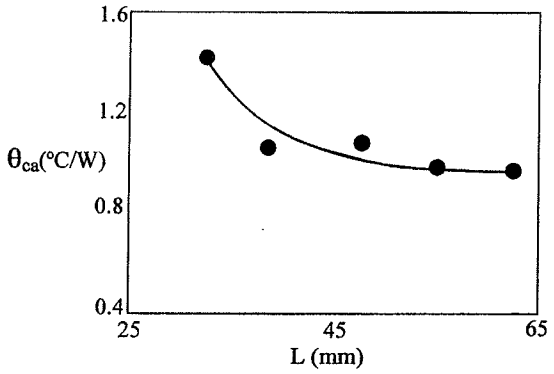

Fig. 8 Effect of fin length on the thermal resistance of the heat sink

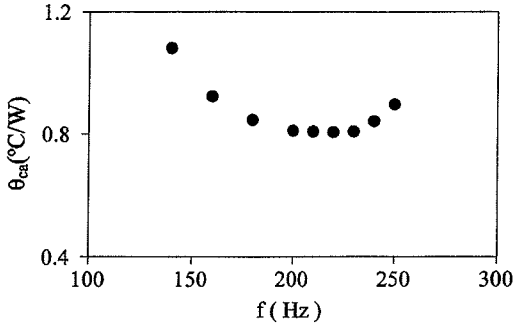

Fig. 10 Effect of actuator frequency on thermal resistance of the heat sink

These results are shown in Fig. 7. A schematic of a single channel is shown on the graph for clarity. For a die temperature of 70°C, the air temperature rises from 24.8 to 60.6°C within a distance of 40 mm from the jet exit. Based on the air temperature rise and the flow rate measured in the previous section, the ideal power that could be dissipated by the heat sink is calculated as 95.7 W from $Q=\rho\hat{U}C_p\Delta T_{ca}$ (where ρ is the density of air, $\hat{U}$ is the volume flow rate through the heat sink, C_p is the specific heat of the fluid, and ΔT_{ca} is the ideal temperature rise of the fluid above the ambient). Since the actual power dissipated is 59.2 W, the thermal effectiveness is 0.62. Beyond a length of 40 mm, the air temperature ceases to rise. This is reflected in the thermal resistance of the heat sink plotted as a function of fin length in Fig. 8, obtained by successively chopping small lengths of the heat sink and measuring the corresponding die temperature and power. As can be seen from the figure the thermal resistance becomes fairly constant after a fin length of about 45 mm, since the air temperature and the fin temperature are equal beyond that.

From the definition of thermal effectiveness, the exit air temperature can be written as a function of case temperature as, $T_e=T_a+\eta\times(T_c-T_a)$. Figure 9 shows the variation in the measured air temperature at the exit of the channels with the case temperature above ambient. The thermal resistance is calculated as 0.61 from the slope of the straight line fit of the data and this value compares very well with that obtained in the previous section. The thermal effectiveness of steady fan driven flows is usually of the order of 0.25. Thus, it is seen that synthetic-jet-based heat sinks have more than two times higher thermal effectiveness when compared to steady flows due to higher heat transfer at low volume flow rates yielded by the inherent small-scale mixing induced by synthetic jets.

Figure 10 shows the effect of varying the actuator frequency (f) on the thermal resistance of the package. Because of the resonance characteristics of the plenum, and the fact that the drivers used in the device have slightly different resonant frequencies, there is a distinct frequency range wherein the thermal resistance is lowest. Away from this frequency range, the drop in thermal performance is not due to change in flow pulsation frequency, but because of lower jet velocity. Nevertheless, the thermal resistance is within 10% of the minimum in the frequency band from 175 to 240 Hz.

3.3 Estimation of the Average Heat Transfer Coeffcients. A simple instrumented heat sink configuration is used to estimate the channel heat transfer coefficients, with thermocouples placed along the length of the fins as well as several locations in the base of the heat sink. The heat sink used for this purpose is similar of that shown in Fig. 2, but does not contain the addition fins in the center of the channels as well as the fin array and jets labeled "2f" in Fig. 2. The channel heat transfer coefficients are calculated based on the energy balance between the heat transferred from the fins to the flow within each channel and the heat transported by the air flowing from the inlet to the exit of the fins. Within each channel the heat transported by the airflow is calculated as $Q=\rho\hat{U}C_p\Delta T_{ea}$ (where ΔT_{ea} is the temperature rise of the fluid above the ambient). The heat transferred from the fin to the mean flow is given by $Q=hA\Delta T_{sf}$ (where h is the heat transfer coefficient to be calculated, A is the internal area of the duct, and ΔT_{sf} is the

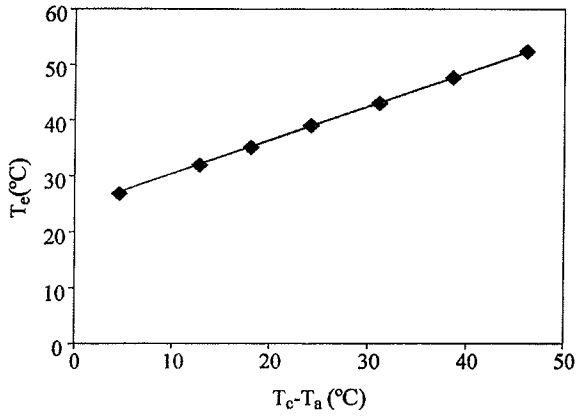

Fig. 9 Variation of exit air temperature with die temperature

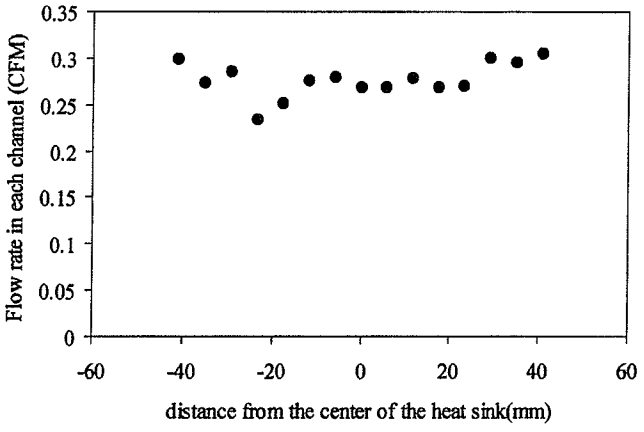

Fig. 11 Volume flow rate within the different channels in the heat sink

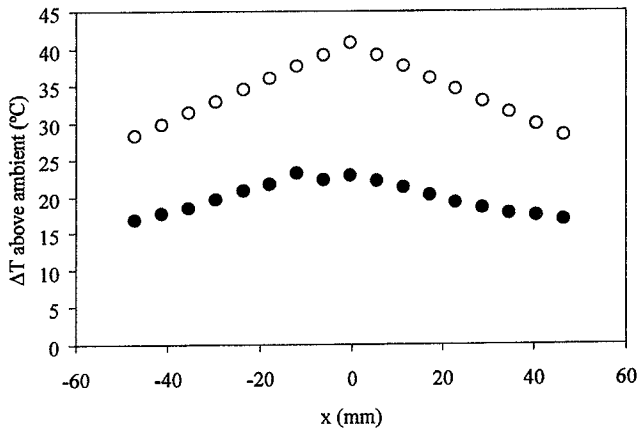

Fig. 12 Variation in fin (○) and exit air temperatures (●) across the channels of the heat sink.

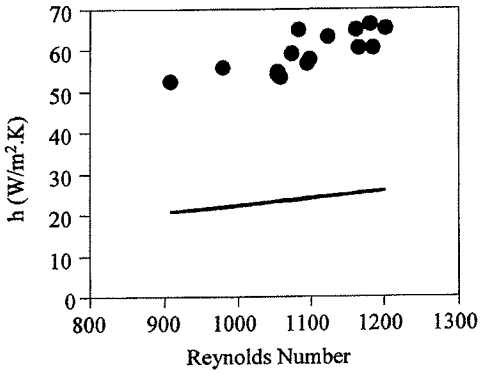

Fig. 13 Comparison of the heat transfer coefficient between synthetic jet ejector channel flow (♦) and empirical correlation for a fully developed steady duct flow (—)

temperature difference between the fins and the local fluid, $T_s - T_f$). From the equivalence of the two heat transports, h is obtained easily since $\hat{U}$, T_e, T_a, T_s, and T_f are known from measurements.

Figure 11 shows the volume flow rate through each channel of the heat sink. The mass flow rates vary from channel to channel due to the slight manufacturing differences in the nozzles. This aspect is utilized to obtain a variation of the heat transfer coefficient as a function of Reynolds number over a small range. The total mass flow rate through the heat sink is 4.44 CFM, resulting in an average of 0.27 CFM per channel.

Figure 12 shows the variation of fin and exit air temperature (T_s and T_e, respectively) across the channels of heat sink. The mean fluid temperature within the channel (T_f) is assumed to be the average of the ambient (inlet) and exit temperatures. As expected, there is almost a linear drop in fin temperature from the center of the heat sink to the outside and since the efficiency and mass flow rate are similar from channel to channel, the exit air temperature follows the same trend. Based on the mass flow rate and the exit air temperature, the average power dissipated within the channels is 1.94 W.

Figure 13 presents the heat transfer coefficient based on these measurements and compares it with empirical correlations for the heat transfer coefficients of flows in ducts (Incropera and Dewitt [16]). For this purpose, each of the channels of the heat sink is considered as a different data point. The heat transfer coefficient achieved with the synthetic jets is around 60 W/m^2 K, which is approximately 2.5 times higher than that achieved with a steady flow (25 W/m^2 K) within a duct for the same Reynolds number. This is attributable to the small-scale vortices and unsteadiness inherent in a synthetic-jet flow. Note that the high thermal effectiveness of the synthetic-jet heat sink is a direct outcome of the higher heat transfer coefficients.

4 Conclusions

The development of an active air-cooled heat sink consisting of a plate-fin heat sink integrated with synthetic-jet actuators is discussed. The synthetic-jet module consists of a plenum driven by electromagnetic actuators operating around 200 Hz. It is found that under natural convection the case-to-ambient thermal resistance of the package is 3.15°C/W. When the synthetic jets are operated, the case temperature decreases from 71.5 to 36°C. The device enables a dissipation of about 59.2 W at 70°C resulting in a case to ambient thermal resistance of 0.76°C/W with synthetic-jet cooling. The jets generate a flow rate of 4.48 CFM through the heat sink, which translates to 0.26 CFM per fin pair. When the same heat sink is tested with synthetic jets and a fan, the synthetic jets dissipate 20–40% higher power in the flow rate range of 3 to 5 CFM. Based on theoretical limits for heat transfer by a given airflow, the efficiency of the synthetic-jet heat sink is 0.61 compared to ≈0.25 for a typical fan-heat-sink. Measurements of the air temperature between the fins of the heat sink show a temperature rise of 35.8°C, indicating the importance of the small-scale heat transfer and mixing induced by the synthetic jets. Due to the resonance characteristics of the plenum and small differences in the resonant frequency of the drivers, there is a 65 Hz band around 200 Hz in which the thermal resistance of the package remains within 10% of the minimum. The heat transfer coefficients generated by the synthetic jets within the channels of the heat sink (~60 W/m^2 K) are 150% higher than those obtained in steady duct flows, resulting in a higher thermal effectiveness of the synthetic-jet ejector heat sink.

Acknowledgments

This work was supported by DARPA's HERETIC Program.

Nomenclature

C_p = specific heat, J/kg K
L = length of the fins of the heat sink (in the mean flow direction), mm
P, Q = power dissipation, W
Re = Reynolds number
T = temperature, °C
V = velocity, m/s
$\hat{U}$ = volume flow rate, CFM
h = heat transfer coefficient, W/m^2 K
x = distance from the center to outer fin of the heat sink, mm
y = distance from the base to the top of the fins, mm
z = distance along the length of the fin, mm (z=0 corresponds to the jet exit)
ρ = density, kg/m^3
θ = thermal resistance, °C/W
η = efficiency

Subscripts

a = ambient
c = case (integrated heat spreader on the die)
e = exit plane of heat sink flow channels
f = fluid within channel
s = fin surface
ca = case-to-ambient
ea = exit-to-ambient
sf = fin surface-to-fluid

References

[1] *International Technology Roadmap for Semiconductors* (Semiconductor Industry Association, Palo Alto, 2001).

[2] Bar-Cohen, A., 2000, "Computer-Related Thermal Packaging at the Millennial Divide," Electronics Cooling, **6**, No. 1, pp. 32–40.

[3] Smith, B. L., and Glezer, A., 1998, "The Formation and Evolution of Synthetic Jets," Phys. Plasmas, **10**, No. 9, pp. 2281–2297.

[4] Glezer, A., and Amitay, M., 2002, "Synthetic Jets," Annu. Rev. Fluid Mech., **34**, pp. 503.

[5] Jambunathan, K., Lai, E., Moss, M. A., Button, B. L., 1992, "A Review of Heat Transfer Data for Single Circular Jet Impingement," Int. J. Heat Fluid Flow, **13**, pp. 106–115.

[6] Lehmann, G. L., and Kosteva, S. J., 1990, "A Study of Forced Convection Direct Air Cooling in the Downstream Vicinity of Heat Sinks," J. Electron. Packag., **112**, pp. 234–240.

[7] Maveety, J. G., and Hendricks, J. F., 1999, "A Heat Sink Performance Study Considering Material, Geometry, Nozzle Placement and Reynolds Number with Air Impingement," J. Electron. Packag., **121**, pp. 156–161.

[8] Slayzak, S. J., Viskanta, R., and Incropera, F. P., 1994, "Effects of Interactions Between Adjoining Rows of Circular, Free-Surface Jets on Local Heat Transfer from the Impingement Surface," J. Heat Transfer, **116**, No. 1, pp. 88–95.

[9] Morris, G. K., and Garimella, S. V., 1998, "Orifice and Impingement Flow Fields in Confined Jet Impingement," J. Electron. Packag., **120**, No. 1, pp. 68–72.

[10] Thompson, M. R., Denny, D. L., Black, W. Z., Hartley, J. G., and Glezer, A., 1997, "Cooling of Microelectronic Devices using Synthetic Jet Technology," 11th European Microelectronics Conference, Venice, Italy, pp. 362–366.

[11] Russell, G. B., 1999, "Local- and System-Level Thermal Management of a Single Level Integrated Module (SLIM) using Synthetic Jets," M. S. thesis, Georgia Institute of Technology, Atlanta, GA.

[12] Mahalingam, R., and Glezer, A., 2001, "An Actively Cooled Heat Sink Integrated with Synthetic Jets," Proceedings of 35th National Heat Transfer Conference, Anaheim, CA.

[13] Mahalingam, R., and Glezer, A., 2001, "Synthetic Jet Based Impingement Cooling Module for Electronic Cooling," Proceedings of the IMAPS 2001 Symposium, Baltimore, MD.

[14] Gosline, J. E., and O'Brien, M. P., 1934, "The Water Jet Pump," Univ. Calif. Publ. Eng., **3**, p. 167.

[15] Winoto, S. H., Li, H., and Shah, D. A., 2000, "Efficiency of Jet Pumps," J. Hydraulic Engineering, **126**, pp. 150–156.

[16] Incropera, F. P., and Dewitt, D. P., "Fundamentals of Heat and Mass Transfer," 3rd ed., Wiley Publishing, New York, pp. 496–502.